Molecular Therapy
Nucleic Acids
Original Article

METTL3-mediated m^{6}A mRNA modification promotes esophageal cancer initiation and progression via Notch signaling pathway

Hui Han,[1,2,5] Chunlong Yang,[1,5] Shuishen Zhang,[3,5] Maosheng Cheng,[1,5] Siyao Guo,[1] Yan Zhu,[1] Jieyi Ma,[1] Yu Liang,[1] Lu Wang,[1] Siyi Zheng,[1] Zhaoyu Wang,[1] Demeng Chen,[1,2] Yi-Zhou Jiang,[4] and Shuibin Lin[1,2]

[1]Center for Translational Medicine, Precision Medicine Institute, The First Affiliated Hospital, Sun Yat-sen University, Guangzhou 510080, China; [2]State Key Laboratory of Oncology in South China, Sun Yat-sen University Cancer Center, Guangzhou 510060, China; [3]Department of Thoracic Surgery, The First Affiliated Hospital, Sun Yat-sen University, Guangzhou 510080, China; [4]Institute for Advanced Study, Shenzhen University, Shenzhen 518057, China

Esophageal cancer is a lethal malignancy with a high mortality rate, while the molecular mechanisms underlying esophageal cancer pathogenesis are still poorly understood. Here, we found that the N6-methyladenosine (m^{6}A) methyltransferase-like 3 (METTL3) is significantly upregulated in esophageal squamous cell carcinoma (ESCC) and associated with poor patient prognosis. Depletion of METTL3 results in decreased ESCC growth and progression *in vitro* and *in vivo*. We further established ESCC initiation and progression models using *Mettl3* conditional knockout mouse and revealed that METTL3-mediated m^{6}A modification promotes ESCC initiation and progression *in vivo*. Moreover, using METTL3 overexpression ESCC cell model and *Mettl3* conditional knockin mouse model, we demonstrated the critical function of METTL3 in promoting ESCC tumorigenesis *in vitro* and *in vivo*. Mechanistically, METTL3-catalyzed m^{6}A modification promotes NOTCH1 expression and the activation of the Notch signaling pathway. Forced activation of Notch signaling pathway successfully rescues the growth, migration, and invasion capacities of METTL3-depleted ESCC cells. Our data uncovered important mechanistical insights underlying ESCC tumorigenesis and provided molecular basis for the development of novel strategies for ESCC diagnosis and treatment.

INTRODUCTION

Esophageal cancers, including esophageal adenocarcinoma (EAC) and esophageal squamous cell carcinoma (ESCC), are malignant tumors that seriously threaten human health.[1,2] Esophageal cancer ranks as the seventh most common cancer worldwide and is a leading cause of cancer-related mortality.[3,4] ESCC represents more than 90% of esophageal cancers and is often diagnosed at advanced stages.[2,5] The high mortality rate of esophageal cancer is due to the lack of the effective diagnosis and therapeutic strategies.[1,2,5] Therefore, better understanding of the molecular mechanisms underlying esophageal cancer pathogenesis is crucial for clinical diagnosis and treatment of esophageal cancer patients.

Abnormal genetic changes and/or epigenetic abnormalities often lead to ESCC pathogenesis.[6–8] Mutations of key cancer genes, including *P53*, *CCND1*, and *NOTCH* receptors, are often associated with ESCC progression.[8] In addition, mis-regulated DNA methylation, histone modifications, and non-coding RNAs also result in mis-regulated gene expression and ESCC development.[7–9] In recent years, mRNA modifications were reported to play essential functions in regulation of posttranscriptional gene expression. N6-methyladenosine (m^{6}A) is the most abundant internal modification on eukaryotic mRNAs.[10,11] Methyltransferase-like 3 and 14 (METTL3 and METTL14) and their cofactors catalyze m^{6}A modification on target mRNAs.[10] In contrast, the m^{6}A demethylases, including FTO and ALKBH5, can remove m^{6}A modification from mRNAs.[11,12] Different types of m^{6}A readers recognize the m^{6}A modification of a given target mRNA and regulate the stability, translation, splicing, or nuclear transport of the target mRNAs.[13–16] Given the important function of m^{6}A modification in gene expression regulation, the mis-regulations of m^{6}A modification often result in developmental diseases and cancers. Our previous studies have shown that the m^{6}A methyltransferase METTL3 enhances the expression of various oncogenes and therefore promotes cancer progression.[13–16] Moreover, recent studies further uncovered the essential functions of m^{6}A mRNA modification in regulation of different cancer types.[17,18] METTL3 is upregulated in ESCC,[19] however, the physiological functions and underlying molecular mechanisms of METTL3-mediated m^{6}A modification in ESCC remain poorly understood.

Received 10 March 2021; accepted 13 July 2021;
https://doi.org/10.1016/j.omtn.2021.07.007.

[5]These authors contributed equally

Correspondence: Demeng Chen, Center for Translational Medicine, Precision Medicine Institute, The First Affiliated Hospital, Sun Yat-sen University, Guangzhou 510080, China.
E-mail: chendm29@mail.sysu.edu.cn
Correspondence: Yi-Zhou Jiang, Institute for Advanced Study, Shenzhen University, Shenzhen 518057, China.
E-mail: jiangyz@szu.edu.cn
Correspondence: Shuibin Lin, Center for Translational Medicine, Precision Medicine Institute, The First Affiliated Hospital, Sun Yat-sen University, Guangzhou 510080, China.
E-mail: linshb6@mail.sysu.edu.cn

In this study, we found that METTL3 expression is upregulated in human esophageal cancer samples and is associated with poor esophageal cancer progression. We further revealed the crucial functions of METTL3-mediated m^{6}A modification in promoting ESCC initiation and progression *in vitro* and *in vivo* through activation of the NOTCH1 signaling pathway. Our work uncovered novel mechanisms underlying ESCC tumorigenesis and could provide new insights for the development of effective therapeutic strategies for ESCC treatment.

RESULTS

METTL3 is elevated in ESCCs and is associated with poor ESCC prognosis

To study the potential functions of METTL3-mediated m^{6}A modification in esophageal cancer, we first determined the METTL3 expression in esophageal cancer patient samples using The Cancer Genome Atlas (TCGA) database (TCGA database: https://portal.gdc.cancer.gov/). Our analysis revealed that METTL3 mRNA expression is significantly upregulated in esophageal tumor tissues compared with those in normal tissues (Figure 1A). In addition, high METTL3 expression is associated with advanced tumor grades and cancer stages (Figures 1B and 1C) and high lymph node metastasis activity of esophageal cancer (Figure 1D). Moreover, patients with higher METTL3 expression have significantly poorer disease-free survival status (Figure 1E). To further verify the association between METTL3 and esophageal cancer progression, we performed immunohistochemistry (IHC) staining of METTL3 on tumor tissues from our cohort of ESCC patients. Consistently, we found a significantly higher expression of METTL3 in ESCC tumor tissues than those in peri-tumor tissues (Figures 1F–1H). Furthermore, data from our cohort also supported that high METTL3 expression is associated with poor prognosis of ESCC patients (Figures 1I and 1J). Overall, these data indicate the important functions of METTL3 in regulation of ESCC progression.

Targeting METTL3 expression impairs ESCC progression

To study the underlying molecular mechanisms of METTL3 in regulation of ESCC, we knocked down METTL3 expression in TE-9 and TE-10 ESCC cells using two distinct short hairpin RNAs (shRNA1 and shRNA2; hereafter referred to collectively as sh1 and sh2). Compared with the non-specific control (NC), both sh1 and sh2 significantly reduced METTL3 protein expression (Figure 2A). Knockdown of METTL3 inhibits proliferation (Figure 2B) and colony formation (Figures 2C and 2D) of ESCC cells, suggesting that METTL3 is essential for the ESCC growth. We further performed wound healing assay and migration assay and found that METTL3 depletion significantly reduces the migration of ESCC cells (Figures 2E–2H). Moreover, cell invasion assay also revealed that knockdown of METTL3 reduces the invasion ability (Figures 2I and 2J) of both TE-9 and TE-10 cells. Collectively, our *in vitro* results uncover the critical role of METTL3 in the regulation of ESCC progression.

METTL3-mediated m^{6}A modification regulates Notch signaling pathway

We next performed m^{6}A methylated RNA immunoprecipitation-sequencing (MeRIP-seq) to identify the downstream target and underlying molecular mechanisms of m^{6}A in regulation of ESCC. Analysis of our m^{6}A MeRIP-seq data revealed that m^{6}A-modified sites are selectively located at the GGAC motif near the translation stop codon (Figures 3A and 3B). Gene Ontology (GO) analysis uncovered that the m^{6}A-modified transcripts are significantly enriched in cancer gene pathways, including the Notch signaling pathway (Figure S1). Moreover, GO analysis of RNA-seq data revealed that the downregulated mRNAs in the METTL3 knockdown ESCC cells are also significantly enriched in the Notch signaling pathway (Figure S2), suggesting the potential function of METTL3 in regulation of Notch pathway in ESCC cells. Key Notch pathway component NOTCH1 receptor has strong and specific m^{6}A modification located near its translation stop codon (Figure 3C). Moreover, gene set enrichment analysis (GSEA) uncovered that depletion of METTL3 in ESCC cells resulted in a significant change of Notch signaling pathway gene expression (Figure 3D; Tables S3 and S4). Notch signaling pathway is an important oncogenic pathway in cancers, therefore, we further studied the function of METTL3-mediated m^{6}A mRNA modification in regulation of Notch pathway in ESCC. Expression analysis revealed that NOTCH1 expression is significantly upregulated in ESCC samples compared with the controls (Figure 3E). Moreover, the expressions of METTL3 and NOTCH1 are significantly correlated (Figure 3F), further confirming the potential role of METTL3-mediated m^{6}A modification in regulation of the Notch signaling pathway in ESCC. We next knocked down METTL3 expression and found that depletion of METTL3 results in decrease of the m^{6}A modification, mRNA, and protein expression levels of NOTCH1; moreover, the expression of Notch target P21 also decreases upon METTL3 depletion (Figures 3G–3I). Overall, our data uncover that METTL3 regulates the m^{6}A modification and the expression of the NOTCH1 receptor in ESCC cells.

Activation of the Notch pathway rescues ESCC progression in METTL3-depleted ESCC cells

To determine whether the Notch signaling pathway is a key downstream target of METTL3 in ESCC, we further performed rescue assay by forced activation of NOTCH1 in the METTL3-depleted cells. As shown in Figures 4A and 4B, overexpression of the active form of NOTCH1 (Intracellular domain of NOTCH1 [ICN1]) increased the expression of NOTCH1 in METTL3 knockdown cells, suggesting that we have successfully activated the Notch signaling pathway. Forced activation of the NOTCH1 signaling pathway rescued the growth (Figure 4C) and colony formation (Figures 4D and 4E) capacities of the METTL3 knockdown ESCC cells. In addition, wound healing (Figures 4F and 4G), migration, and invasion (Figures 4H and 4I) assays further revealed that NOTCH1 activation significantly promoted the migration and invasion of METTL3-depleted ESCC cells. These data support that the NOTCH1 signaling pathway is an important downstream target of METTL3 and is essential for its function in promoting ESCC progression.

Knockout (KO) of *Mettl3* inhibits ESCC initiation *in vivo*

We next generated the Keratin14 promoter-driven *Mettl3* conditional knockout (*Keratin14-CreER; Mettl3$^{fl/fl}$*, cKO) mouse model to study

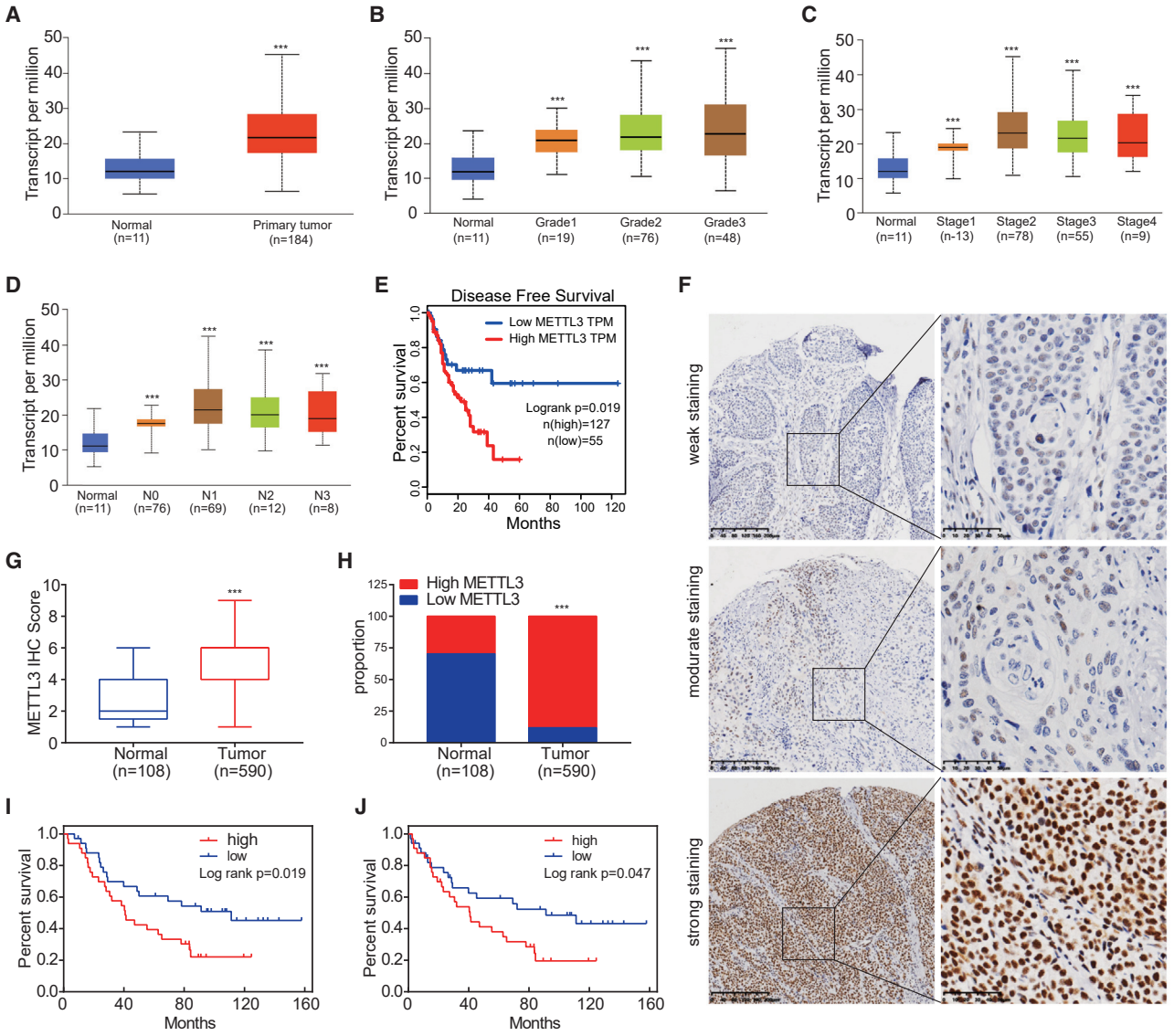

Figure 1. METTL3 is elevated in ESCCs and is a negative prognostic factor for ESCC patients

(A) Quantification of METTL3 expression (transcripts per million [TPM]) in normal esophageal tissues and primary esophageal tumor. (B) METTL3 expression level in normal esophageal tissues and different grades of esophageal tumor tissues. (C) METTL3 expression level in normal esophageal tissues and different stages of esophageal tumor tissues. (D) METTL3 expression level in normal esophageal tissues and tumor tissues with different stages of lymph node metastasis. (E) Disease-free survival of ESCC patients with high or low METTL3 expression level. Kaplan-Meier was employed to analyze the survival fraction. (F and G) IHC staining of METTL3 in clinical samples and the quantification of METTL3 staining scores. (H) Proportion of high/low METTL3 expression cases in tumor tissues and the adjacent normal tissues. (I and J) Correlation between METTL3 expression and overall survival (I) or disease-free survival (J) of ESCC patients. Data are represented as means ± SDs. *$p < 0.05$, **$p < 0.01$, ***$p < 0.001$ (Student's t test; Dunnett's test; log rank test).

the function of METTL3 in regulation of ESCC initiation and progression *in vivo*. To determine the role of Mettl3 in regulation of ESCC initiation, we first induced *Mettl3* cKO by tamoxifen injection and then subjected the *Mettl3* cKO and control mice to 16 weeks of 4-nitroquinoline N-oxide (4NQO) treatment to induced ESCC formation. On week 21, the mice were sacrificed for analysis of ESCC tumorigenesis in the *Mettl3* cKO and control mice (Figures 5A and 5B). As shown in Figure 5C, *Mettl3* cKO resulted in fewer and smaller lesions in the esophagus of mice compared with those in the control mice. Significantly decreased tumor burden as indicated by the reduced visible lesion area was observed on cKO mice (Figure 5D). Correspondingly, hematoxylin and eosin (H&E) staining revealed that *Mettl3* cKO mice have a significantly decreased number of dysplasias and squamous cell carcinomas than those in the control

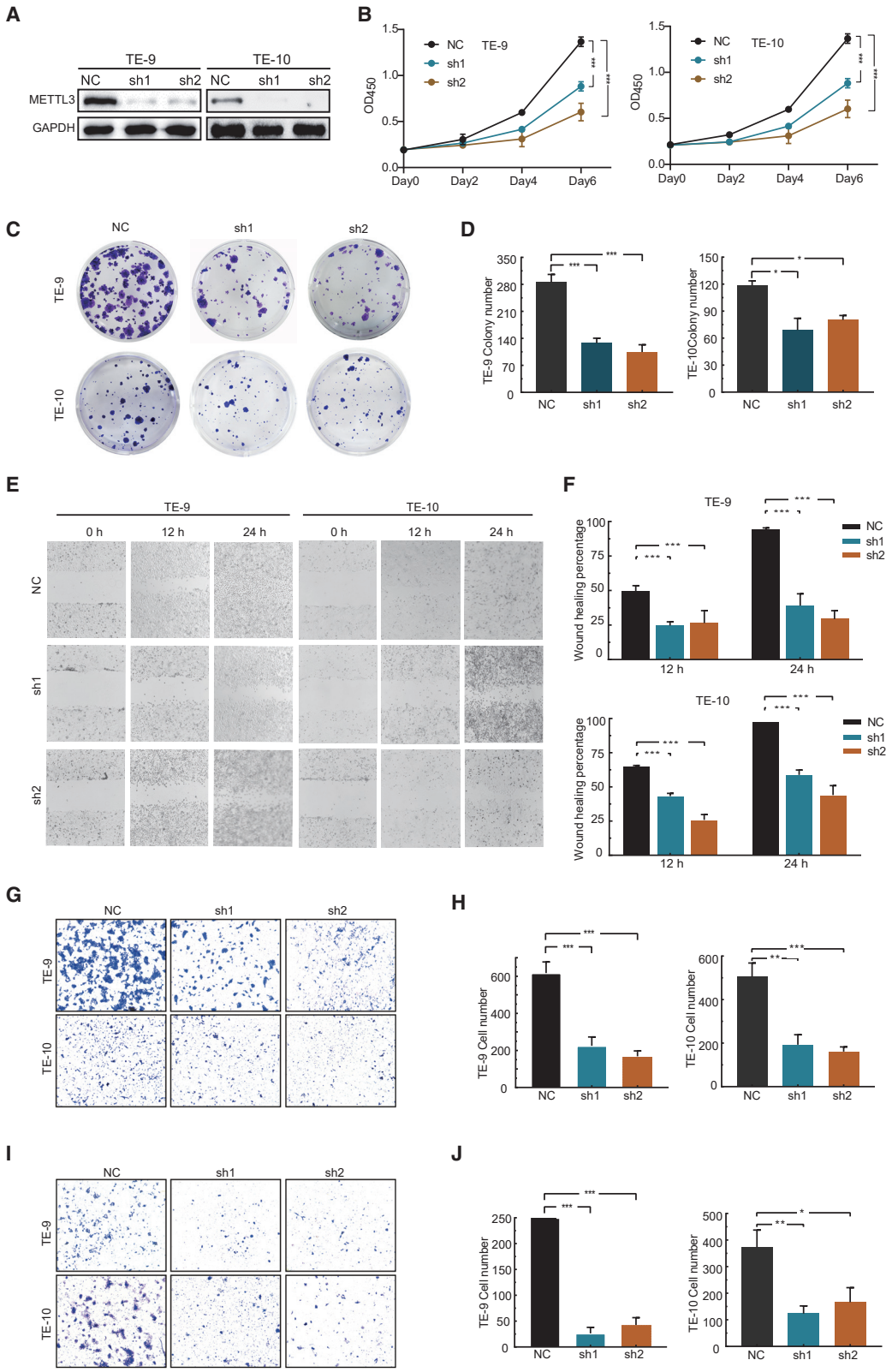

(legend on next page)

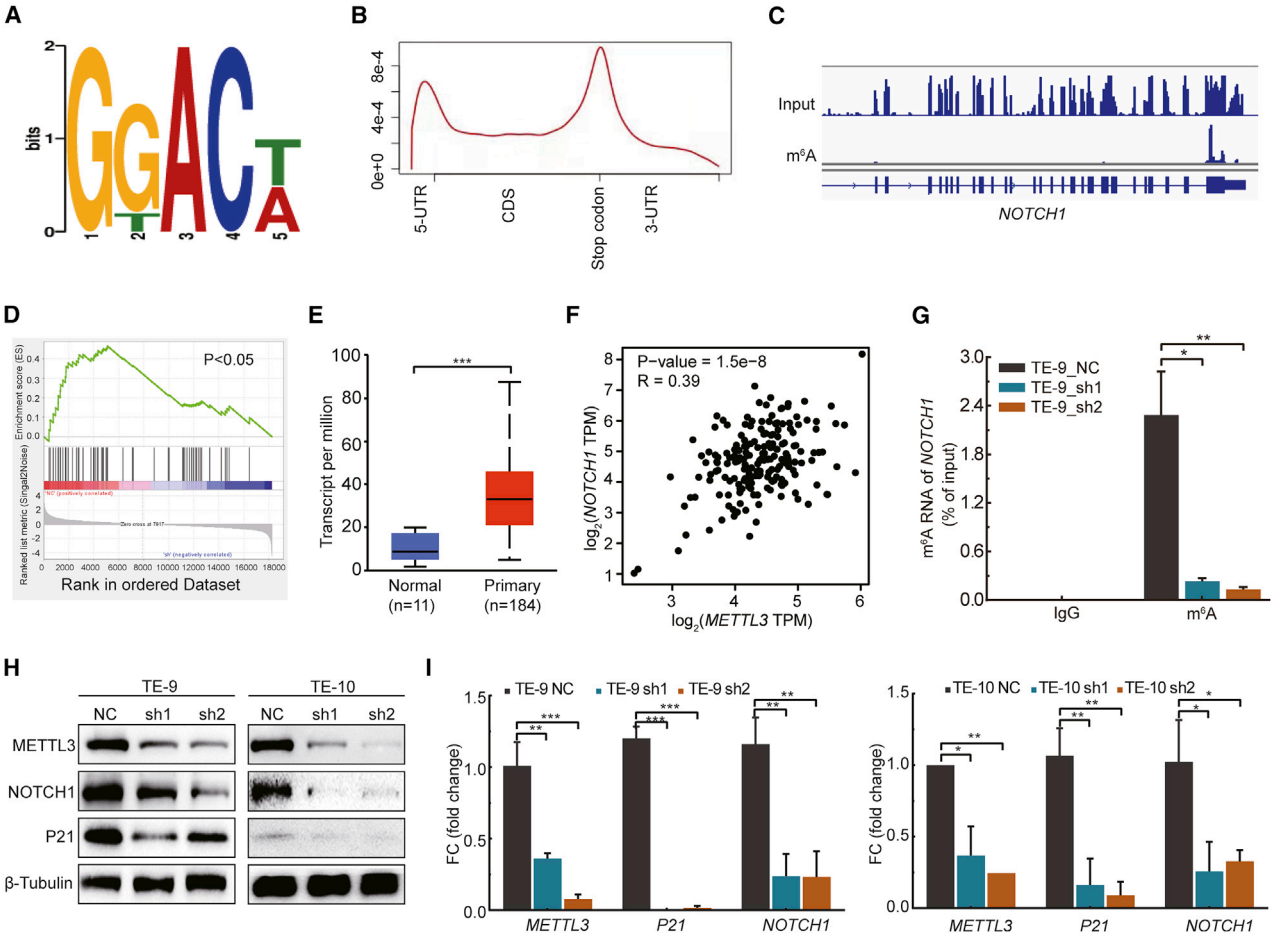

Figure 3. METTL3-mediated m^{6}A modification regulates the Notch signaling pathway

(A) The sequence motif for m^{6}A methylation identified in ESCC cells. (B) Metagene profiles of m^{6}A distribution across the transcriptome in ESCC cells. (C) Representative m^{6}A modification of NOTCH1 in ESCC cells. (D) GSEA analysis of transcriptome in NC cells or shMETTL3 cells with gene set from Notch signaling pathway. (E) Quantification of NOTCH1 expression (transcripts per million [TPM]) in normal esophageal tissues and primary esophageal tumor. (F) Correlation analysis of METTL3 and NOTCH1 expression in ESCC using TCGA database. (G) m^{6}A-MeRIP-qPCR analysis showed the m^{6}A level of *NOTCH1* in ESCC cells with or without METTL3 knockdown. (H) Western blot of NOTCH1 and P21 protein level in METTL3-depleted ESCC cells. (I) qRT-PCR analysis of *NOTCH1* and *P21* mRNA level in METTL3-depleted ESCC cells. Data are represented as mean ± SD. *p < 0.05, ***p < 0.001 (one-way ANOVA; Student's t test; chi-square test).

mice (Figures 5E–5G). IHC staining further uncovered that the Ki67, NOTCH1, and HES1 expression levels are significantly decreased in the ESCC derived from the *Mettl3* cKO mice (Figures 5H–5K), suggesting that *Mettl3* cKO decreased the NOTCH1 signaling pathway activity and reduced the proliferation of ESCC *in vivo*. Interestingly, the expression of ESCC cancer stem cell marker SOX2 also decreased in the *Mettl3* cKO mice (Figures S3A and S3B), suggesting that METTL3-mediated m^{6}A modification could regulate the cancer stem cell function *in vivo*. Overall, these results support the critical function of METTL3 for the *in vivo* ESCC initiation.

Mettl3 is essential for ESCC progression *in vivo*

We further established an *in vivo* ESCC progression model to determine the role of METTL3 in ESCC progression using the *Mettl3* cKO mice. Here we first treated the *Keratin14-CreER; Mettl3$^{fl/fl}$* and control mice with 4NQO for 16 weeks to induce ESCC formation. After

Figure 2. Targeting METTL3 expression impairs progression of ESCC *in vitro*

(A) Western blotting confirmation of METTL3 knockdown in TE-9 and TE-10 cells. (B) Growth of NC or shMETTL3 cells evaluated by CCK8. (C and D) Colony formation assay (C) and the quantification data (D) of TE-9 and TE-10 cells with or without METTL3 knockdown. (E and F) Wound healing assay (E) and the quantification data (F) of TE-9 and TE-10 cells with or without METTL3 knockdown. (G and H) Invasion assay (G) and the quantification data (H) of TE-9 and TE-10 cells with or without METTL3 knockdown. (I and J) Migration assay and the quantification data (J) of TE-9 and TE-10 cells with or without METTL3 knockdown. Data are represented as mean ± SD. *p < 0.05, **p < 0.01, ***p < 0.001 (one-way ANOVA; Student's t test).

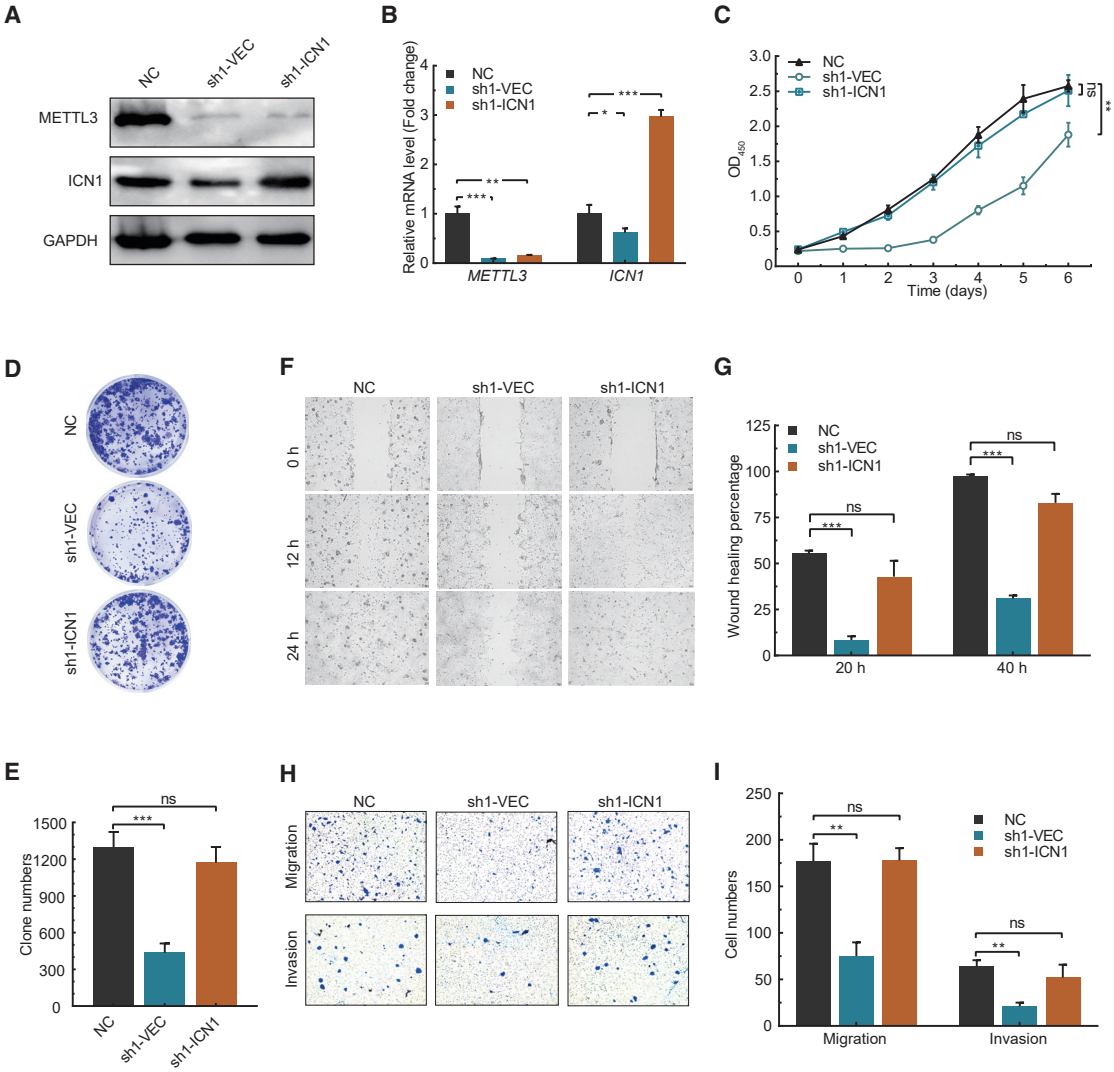

Figure 4. Activation of Notch pathway rescues ESCC progression in METTL3-depleted cells

(A) Western blot of ICN1 expression in METTL3-depleted ESCC cells. (B) qRT-PCR of ICN1 expression in METTL3-depleted ESCC cells. (C) CCK8 assay of METTL3-depleted ESCC cells with or without ICN1 overexpression. (D and E) Colony formation assay (D) and the quantification data (E) of METTL3-depleted ESCC cells with or without ICN1 overexpression. (F and G) Wound healing assay (F) and the quantification data (G) of METTL3-depleted ESCC cells with or without ICN1 overexpression. (H and I) Migration and invasion assay (H) and the quantification data (I) of METTL3-depleted ESCC cells with or without ICN1 overexpression. Data are represented as mean ± SD. *$p < 0.05$, ***$p < 0.001$ (one-way ANOVA; Student's t test).

that, all the mice with the same condition of tumor bearing were injected with tamoxifen to induce *Mettl3* cKO in the cKO mice, which allows us to study the function of METTL3 in regulation of the pre-existing ESCC *in vivo* (Figures 6A and 6B). At week 21, the mice were sacrificed for analysis of METTL3's function in *in vivo* ESCC progression. Our data revealed that *Mettl3* cKO in the tumor-bearing mice resulted in slower progression and milder tumor symptoms, as shown by the decreased visible lesion area in the cKO mice compared with those in the control mice (Figures 6C and 6D). In addition, *Mettl3* cKO in mice with pre-existing ESCC significantly decreased the number of dysplasias and squamous cell carcinomas (Figures 6E–6G). Furthermore, KO of Mettl3 also resulted in the reduced Ki67 expression and NOTCH1 signaling pathway activity in the ESCC (Figures 6H–6K), suggesting that 3METTL3 is essential for the NOTCH1 activation and proliferation activity of the ESCC *in vivo*. Overall, these data support the essential function of METTL3 in promoting the progression of ESCC *in vivo*.

Overexpression of METTL3 promotes ESCC tumorigenesis *in vitro* and *in vivo* in *Mettl3* transgenic mice

Given that METTL3 expression is significantly upregulated in human ESCC samples, we determined whether overexpression of METTL3

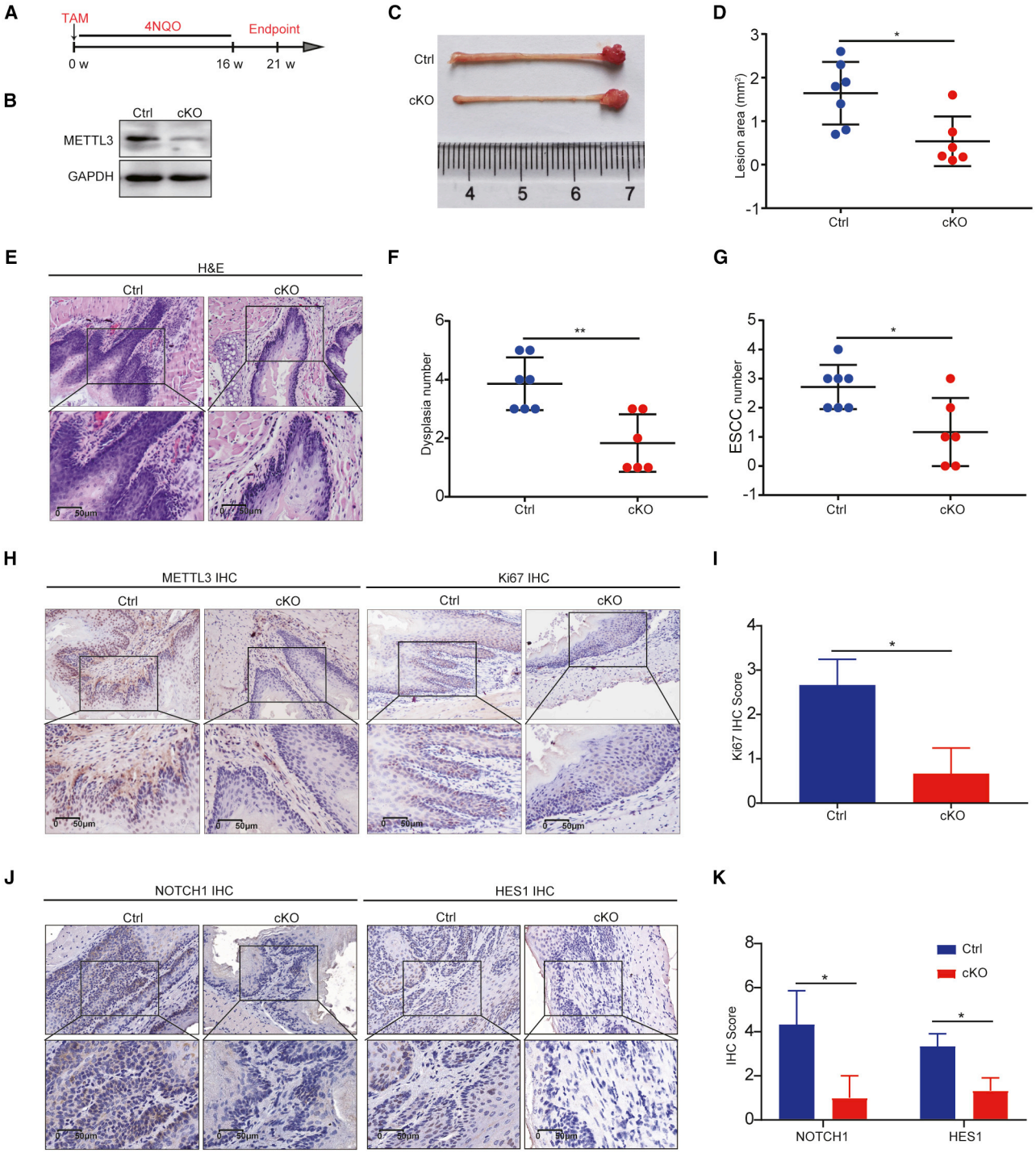

Figure 5. Knockout of *Mettl3* inhibits occurrence of ESCC *in vivo*

(A) Experimental design for inducing mouse ESCC by 4NQO with or without epithelium-specific conditional *Mettl3* KO. Keratin14-Cre was activated before the treatment of 4NQO. (B) Western blot with METTL3 antibody. (C) Representative image of esophageal lesions 21 weeks after 4NQO treatment. (D) Quantification of lesion areas in control group and cKO group. (E) Representative H&E staining of esophagus tissues in control group and cKO group. (F) Quantification of dysplasia numbers in control group and cKO group. (G) Quantification of ESCC numbers in control group and cKO group. (H) Representative images of METTL3 and Ki67 IHC staining of esophagus tissues in control group and cKO group. (I) Quantification of Ki67 staining scores in control group and cKO group. (J) Representative images of NOTCH1 and HES1 IHC staining in control group and cKO group. (K) Quantification of NOTCH1 and HES1 staining scores in control group and cKO group. Ctrl, control. Data are represented as mean ± SD. *$p < 0.05$, **$p < 0.01$, ***$p < 0.001$ (Student's t test).

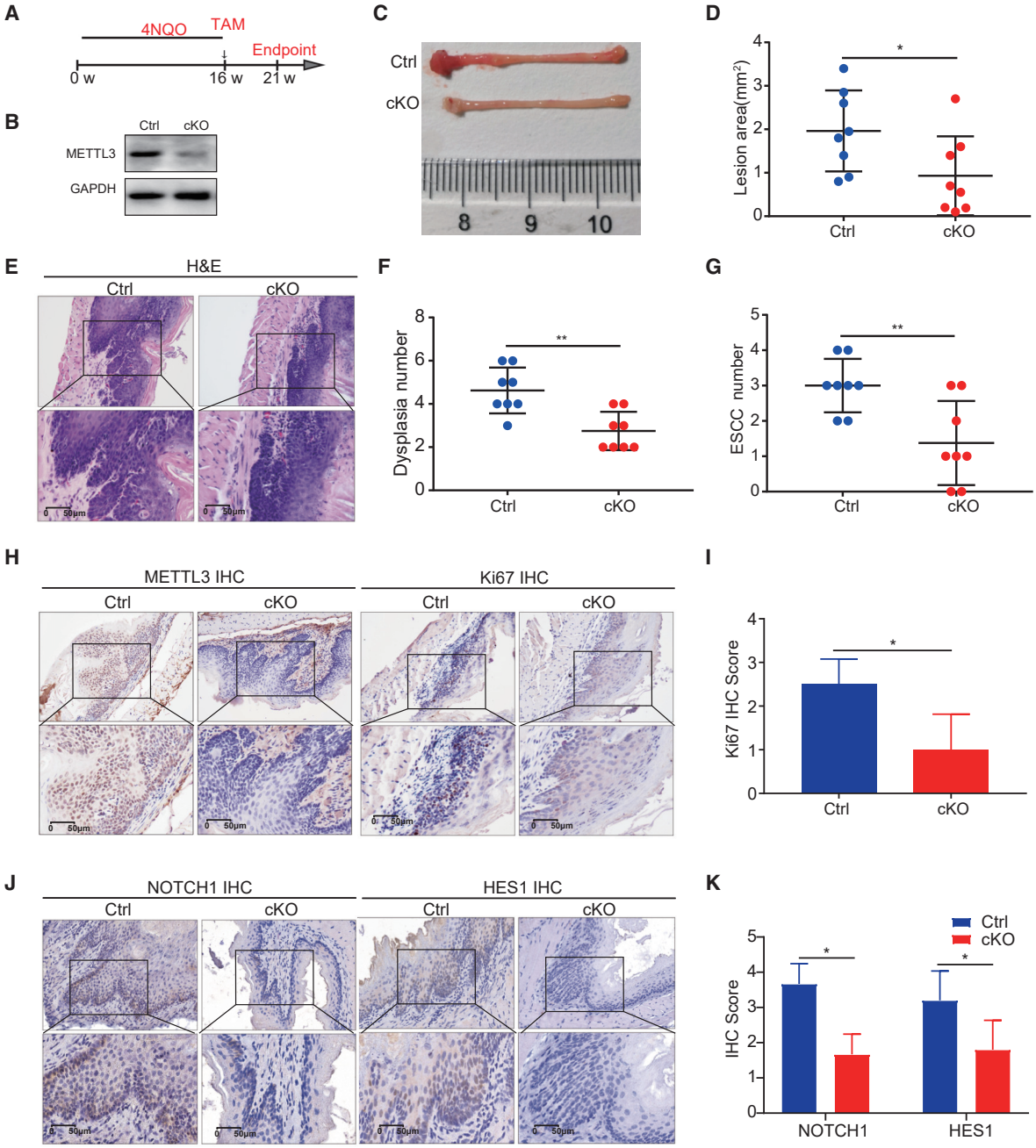

Figure 6. Knockout of *Mettl3* inhibits progression of ESCC *in vivo*

(A) Experimental design for inducing mouse ESCC by 4NQO with or without epithelium-specific conditional *Mettl3* knockout. Keratin14-Cre was activated after the treatment of 4NQO for 16 weeks. (B) Western blot with METTL3 antibody. (C) Representative image of esophageal lesions 21 weeks after 4NQO treatment. (D) Quantification of lesion areas in esophageal tissues with or without *Mettl3* cKO. (E) Representative H&E staining of esophagus in control group and cKO group. (F) Quantification of dysplasia numbers in control group and cKO group. (G) Quantification of ESCC numbers in control group and cKO group. (H) Representative images of METTL3 and Ki67 IHC staining of esophageal tissues in control group and cKO group. (I) Quantification of Ki67 staining scores of esophageal tissues in control group and cKO group. (J) Representative images of NOTCH1 and HES1 IHC staining of esophageal tissues in control group and cKO group. (K) Quantification of NOTCH1 and HES1 staining scores of esophageal tissues in control group and cKO group. Ctrl, control. Data are represented as mean ± SD. *$p < 0.05$, **$p < 0.01$, ***$p < 0.001$ (Student's t test).

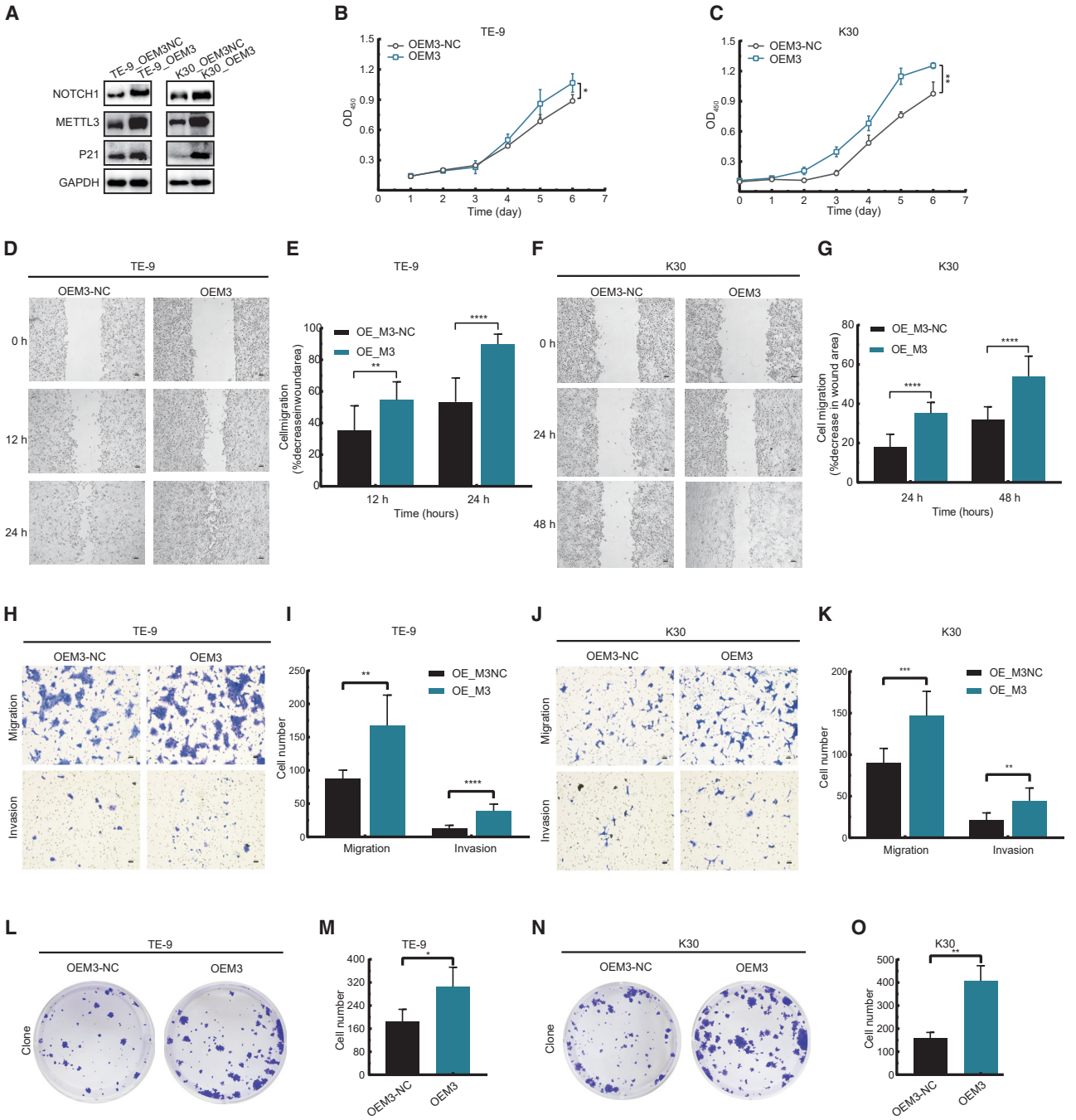

Figure 7. Overexpression of METTL3 promotes ESCC progression *in vitro*

(A) Western blot with indicated antibodies of METTL3 overexpressed (OEM3) TE-9 and KYSE-30 cells. (B and C) Proliferation of OEM3 TE-9 cells (B) and KYSE-30 cells (C) by CCK8 assay. (D–G) Wound healing assay of migration ability OEM3 TE-9 cells (D and E) and KYSE-30 cells (F and G). (H–K) Transwell assay of OEM3 TE-9 cells (H and I) and KYSE-30 cells (J and K). (L–O) Colony formation assay of OEM3 TE-9 cells (L and M) and KYSE-30 cells (N and O). Data are mean ± SD. *p < 0.05; **p < 0.01; ***p < 0.001 against control group (Student's t test).

could promote ESCC progression. Our data revealed that overexpression of METTL3 promotes the expression of NOTCH1 in ESCC cells (Figure 7A). Functionally, METTL3 overexpression promotes the proliferation of ESCC cells, as shown by the Cell Counting Kit-8 (CCK8) assays (Figures 7B and 7C). In addition, overexpression of METTL1 promotes the migration, invasion, and colony formation

capacities of ESCC cells (Figures 7D–7O), further supporting the essential function of the METTL3-m^{6}A-NOTCH1 axis in ESCC regulation of progression.

We further generated the *Mettl3* conditional knockin (cKI) mouse model to study the role of METTL33 in ESCC tumorigenesis *in vivo*. The Keratin14-cre mouse was crossed with *Mettl3*$^{ki/WT}$ mouse to generate the epithelium-specific overexpression of the METTL3 mouse model (*Keratin14-Cre; Mettl3*$^{ki/WT}$, cKI). Then the Mettl3 cKI and control mice were treated with 4NQO for 16 weeks to induce ESCC tumorigenesis (Figures 8A and 8B). At week 20, the mice were sacrificed to study the role of METTL3 overexpression in ESCC tumorigenesis *in vivo*. Our data revealed that Mettl3 cKI mice developed massive tumor burden in esophagus, while only lighter tumor burden occurred in the esophagus of control (Ctrl) mice at week 20 (Figure 8C). The tumor burden as indicated by the visible lesion area in Mettl3 cKI mice was significantly increased compared with that in control mice (Figure 8D). H&E staining revealed that the cKI mice had a significantly increased number of dysplasias and squamous cell carcinomas compared with those in the control mice (Figures 8E–8G), which indicated that forced expression of METTL3 leads to increased tumorigenesis of ESCC. We then performed histological analysis upon the esophagus derived from the two groups of mice. IHC staining uncovered the significant upregulation of METTL3 and Ki67 levels in the cKI mice (Figures 8H and 8I), indicating that the tumors from the cKI mice are more aggressive. Moreover, the expressions of NOTCH1, HES1 and SOX2 are significantly upregulated in the Mettl3 cKI mice (Figures 8J, 8K, S3C, and S3D), confirming that METTL3 activates the NOTCH1 signaling pathway in ESCC *in vivo*. Overall, our data demonstrate the strong function of METTL3 in promoting ESCC tumorigenesis *in vivo*.

DISCUSSION

Here we uncovered that the m^{6}A methyltransferase METTL3 is significantly upregulated in ESCC and associated with poor ESCC prognosis. Our data revealed that depletion of METTL3 decreases human esophageal carcinoma cells' proliferation, invasion, and migration capacities, while overexpression of METTL3 promotes ESCC progression *in vitro*. Most importantly, our *in vivo* ESCC models using epithelium-specific *Mettl3* knockout and knockin mice further supported the strong physiological functions of METTL3 in ESCC occurrence and progression *in vitro*. Mechanistically, we found that the NOTCH1 signal pathway is a crucial m^{6}A target that facilitates METTL3's function in ESCC progression. Overall, our work provided strong *in vitro* and *in vivo* evidence supporting the important function of m^{6}A in the regulation of ESCC tumorigenesis and progression.

Studies in the past few years have revealed that m^{6}A modification plays a key role in different bioprocesses, including RNA processing, tissue development, DNA damage or heat shock responses, circadian clock control, spermatogenesis, maternal-to-zygotic transition, angiogenesis, as well as self-renewal and differentiation of embryonic stem cells.[20–22] More recently, extensive efforts have been made to study the biological impacts of dysregulated m^{6}A modification and the related mechanisms in various cancers. Emerging evidence supported that m^{6}A modification on mRNAs can promote the development and progression of cancers, such as bladder cancer, lung cancer, and breast cancer.[16,23–26] Here we revealed the important oncogenic function of METTL3 in regulation of ESCC *in vitro* and *in vivo*. Most importantly, we established an *in vivo* ESCC tumor model using *Mettl3* cKO and cKI mouse models to provide direct and strong evidence supporting the critical function of METTL3 ESCC initiation and progression.

Mechanistically, we uncovered that the NOTCH1 signaling pathway is a critical m^{6}A target that mediates METTL3's function in promoting ESCC progression. The Notch signaling pathway is a highly conserved pathway that regulates many aspects of cancer biology.[27] NOTCH1 is significantly upregulated in ESCC, and mis-regulation of the Notch pathway promotes ESCC initiation and progression; therefore, targeting the Notch pathway is a promising therapeutic strategy for the treatment of ESCC.[28–30] METTL3-mediated m^{6}A modification could regulate downstream mRNA's splicing, transport, stability, and translation. Our data revealed that *NOTCH1* mRNA has strong and specific m^{6}A modification, and knockdown of METTL3 reduces the mRNA levels of *NOTCH1*, suggesting that METTL3-mediated m^{6}A modification regulates the stability of *NOTCH1* mRNA. Furthermore, we found that forced activation of the NOTCH1 pathway can rescue the growth, migration, and invasion capacities of METTL3 knockdown cells, suggesting that METTL3-mediated m^{6}A modification promotes ESCC progression by regulation of the Notch signaling pathway.

Overall, we demonstrate strong *in vitro* and *in vivo* evidence supporting the critical function of METTL3-mediated m^{6}A modification in promoting ESCC initiation and progression. Our data uncovered novel molecular mechanisms regulating the ESCC pathogenesis and provided new insights for the development of effective therapeutic strategies for ESCC treatment.

MATERIALS AND METHODS

Animals

All animal care and experiments protocols were approved by the Institutional Ethics Committee for Clinical Research and Animal Trials of the First Affiliated Hospital, Sun Yat-sen University. The study was in compliance with all relevant ethical regulations regarding Reporting of *In Vivo* Experiments (ARRIVE) guidelines. Mice were euthanized when they met with the institutional euthanasia criteria for tumor size and overall health condition. Experiments were carried out using mixed male and female animals.

Clinical samples

Paraffin-embedded specimens of tumor and peri-tumor tissues from patients with esophageal carcinoma in this study were obtained from Sun Yat-sen University Cancer Center (Guangzhou, China). Ethical approval for research on human subjects was obtained from the Institutional Review Board of Sun Yat-sen University Cancer Center, and written consent was obtained from all patients prior to analysis.

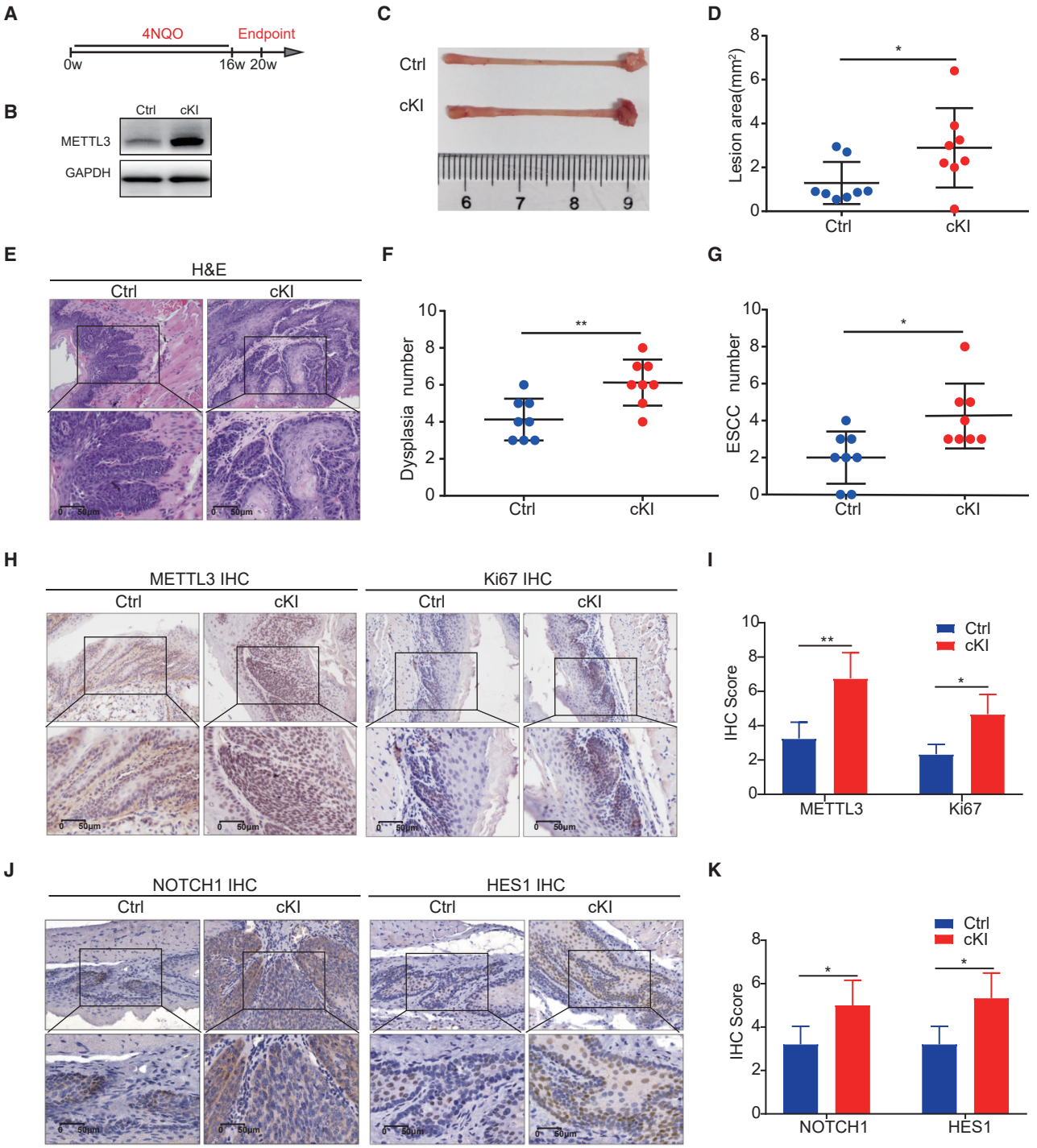

Figure 8. Knockin of *Mettl3* promotes *in vivo* ESCC tumorigenesis

(A) Experimental design for inducing mouse ESCC by 4NQO with or without epithelium-specific *Mettl3* knockin. (B) Western blot with METTL3 antibody. (C) Representative image of esophageal lesions 20 weeks after 4NQO treatment. (D) Quantification of lesion areas in control group and cKI group. (E) Representative H&E staining of esophagus tissues in control group and cKI group. (F and G) Quantification of dysplasia numbers (F) and ESCC numbers (G) in esophagus with or without *Mettl3* cKI. (H) Representative images of 3METTL3 and Ki67 IHC staining in esophageal tissues with or without Mettl3 cKI. (I) Quantification ofMETTL3 and Ki67 staining scores in control group and cKI group. (J) Representative images of NOTCH1 and HES1 IHC staining in control group and cKI group. (K) Quantification of NOTCH1 and HES1 staining scores in control group and cKI group. Ctrl, control. Data are represented as mean ± SD. *$p < 0.05$, **$p < 0.01$, ***$p < 0.001$ (Student's t test).

Cell culture

All the cells were cultured in DMEM (GIBCO, USA) with 10% fetal bovine serum (FBS; GIBCO, USA), 1% streptomycin (GIBCO, USA), and 1% penicillin (GIBCO, USA). Cells were cultured in a water-saturated atmosphere under 5% CO_2 at 37°C.

IHC

Paraffin sections with a thickness of 5 μm were baked for 1 h at 65°C. Prior to immunostaining, paraffin sections were deparaffinized and rehydrated in an alcohol series, followed by antigen retrieval with microwave (MW) heating in Citrate Antigen Retrieval Solution. Sections were blocked with 5% normal goat serum and incubated with the primary antibodies against METTL3 or Ki67 at 4°C overnight. Then immunoreactions were detected with an UltraSensitive S-P Ultrasensitive Kit (horseradish peroxidase [HRP], anti-rabbit) and visualized with 3, 3' -Diaminobenzidine (DAB) substrate. Images were acquired with a microscope (ZEISS, Germany). The protein expression level was evaluated by a semiquantitative immunoreactivity scoring system. The staining intensity was scored as 0 (absent), 1 (weak), 2 (moderate), and 3 (strong), and the proportion of positive staining cells was scored as 0, 1, 2, and 3 for absent, <10%, 10%–50%, and >50%, respectively. The product of intensity score and proportion score resulted in an immunoreactivity scoring system index and was used to evaluate the immunoreactivity of METTL3.

Lentiviral transduction

Lentiviral vectors expressing pLKO.1 shRNAs targeting GFP and METTL3 were obtained from Open Biosystems, Inc. The lentiviral vectors were co-transfected with packaging vector pCMVΔR8.9 and enveloped vector pCMV-VSVG into 293T cells using Lipofectamine 2000 reagent (Invitrogen, USA) for lentivirus production. Viruses were collected to infect TE-9 and TE-10 cells with 8 μg/mL Polybrene (Solarbio, China). The stable infected cells were selected with puromycin (Solarbio, China) (3 μg/mL) for 48 h. The sequences of shRNAs used in this study were listed in Table S1.

Plasmid construction

METTL3 expression plasmid was generated by cloning the full-length open reading frame (ORF) of human METTL3 gene (GenBank: NM_019852.5) into pFLAG-CMV2 vector as previously described.[15] Overexpression of METTL3 was performed using Lipofectamine 2000 reagent (Invitrogen, USA) following the manufacturer's instructions.

RNA isolation and qRT-PCR

RNA isolation and qRT-PCR were performed as previously described.[31] In brief, total RNA was extracted using TRIzol (Invitrogen) according to the manufacturer's instructions. Reverse transcription was performed with PrimeScript RT reagent Kit (Takara, Japan) using 2 μg total RNA in a 20-μL reaction system. After reverse transcription, the cDNA samples were diluted by 1:20 for the analysis of gene expression using qRT-PCR. qRT-PCR was carried out by TB Green Premix Ex Taq II (Takara, Japan) in StepOnePlus real-time PCR system (Thermo Scientific, USA). Each sample was replicated three times, and relative mRNA expression was calculated using *β-ACTIN* as an internal control. Primers used in this study were listed in Table S1.

m^{6}A MeRIP-seq and MeRIP qRT-PCR

The m^{6}A MeRIP-seq and MeRIP qRT-PCR assays were performed as previously described.[15] In brief, total RNA was fragmented using $ZnCl_2$ and incubated with anti-m^{6}A polyclonal antibody (202003; SynapticSystems) at 4°C for 2 h and then treated with protein A/G magnetic beads (88802; Thermo Fisher Scientific) at 4°C for an additional 2 h. The bound RNA was purified and then used for sequencing library construction and qRT-PCR. The library was sequenced with the Illumina Next-Seq 500 sequencer and analyzed as previously described.[15] Methylated sites on RNAs (peaks) were identified with Model-based Analysis of ChIP-Seq (MACS) software.

Western blotting analysis

SDS loading buffer was added to samples and boiled for 5 min at 95°C. Samples were loaded on 10% SDS-PAGE gels and performed with electrophoresis followed by transfer to polyvinylidene fluoride membrane subjected to immunoblotting with different antibodies. After incubation with HRP-conjugated secondary antibodies (CST) at room temperature for 2 h, immunoreactions were visualized using ECL Plus (Thermo Scientific, USA). Antibodies used in this study were listed in Table S2.

Cell proliferation assay

Fifteen hundred cells were seeded into the well of a 96-well culture plate and cultured in 100 μL of culture medium in a humidified, 5% CO_2 atmosphere. CCK8 Reagent (Dojindo, Japan) was used to detect cell proliferation following the manufacturer's instructions. The plate was incubated at 37°C for 1.5 h in a humidified, 5% CO_2 atmosphere. Finally, the absorbance was recorded at 450 nm using an Automatic microplate reader (Bio-Tek, USA).

Clone formation assay

Five hundred cells were seeded in six-well plates with 2 mL fresh medium and grown for 2 weeks. Visible colonies were stained with 0.1% crystal violet, and colony numbers were calculated.

Wound healing assay

One million cells were seeded into the well of six-well culture plates in 3 mL culture medium with FBS and culture until confluent. Use a pipette tip to make a straight scratch in each well, and replace the medium by DMEM (GIBCO, USA) without FBS. Count and record the width of the scratch at 0, 12, and 24 h under a microscope (Leica, Germany).

Cell migration assay

Migration assays were performed using 24-well Transwell inserts with an 8-μm pore size (Corning, USA). One hundred thousand cells in 200 μL of culture medium without FBS were plated in the upper chambers, and 600 μL of culture medium containing 20% FBS was

placed in each bottom chamber. After incubation for 24 h at 37°C, the invaded cells were fixed with 100% methanol for 20 min and stained with 0.1% crystal violet solution for 15 min at room temperature. The invaded cells were counted and recorded under a microscope (Leica, Germany).

Cell invasion assay

Transwell Matrigel invasion assays were performed using 24-well Transwell inserts with an 8-μm pore size (Corning, USA). A 24-well permeable support plate was coated with 200 μg/mL Corning Matrigel matrix (Corning, USA) followed by incubation at 37°C for 5 h to solidify the matrigel matrix. The following steps beginning with seeding cells were performed as cell migration assay.

GO and pathway analysis

GO analysis was performed as previously described.[31] In brief, GO of TE-decreased genes was conducted using the ToppFun module of the ToppGene Suite (https://toppgene.cchmc.org/enrichment.jsp). The ontology terms with Benjamini-Hochberg adjusted p value (false discovery rate [FDR]) < 0.05 were considered as significantly enriched. Pathway analysis was conducted using the GSEA toolkit by pidpathway.

Generation of epithelium-specific conditional *Mettl3* cKO/cKI mice

K14-Cre mice or *K14-CreER* mice were crossed with $Mettl3^{ki/ki}$ or $Mettl3^{fl/fl}$ mice to obtain *K14-Cre;* $Mettl3^{ki/WT}$ mice and *K14-CreER;* $Mettl3^{fl/WT}$ as heterozygous epithelial-specific *Mettl3* cKI mice or heterozygous epithelial-specific *Mettl3* cKO mice. The mice were further crossed to generate *K14-CreER;* $Mettl3^{fl/fl}$ mice, which were ready for experiment. The genotypes of transgenic mice were identified by PCR amplification of target DNA and agarose gel electrophoresis. Genomic DNA was extracted from mouse tails by Mouse Tail Direct PCR Kit (Foregene, China). Primers for floxed *Mettl3* cKO/cKI allele genotyping were listed in Table S1.

ESCC tumorigenesis mouse models

For induction of ESCC, 4-week-old mice were treated with drinking water containing 50 μg/mL 4NQO (Sigma-Aldrich, USA) for 16 weeks and then given normal drinking water for another 4–5 weeks. Cre was activated by the intraperitoneal injection of tamoxifen (Sigma-Aldrich, USA) at a dose of 9 mg per 40 g body weight every other day for a total of three injections. For tumor measurement, mice were sacrificed, and the esophagus was dissected immediately. The surface areas of tumors were measured as described previously.[14] Intact esophagus was fixed in 4% paraformaldehyde for 48 h, embedded in paraffin, and sectioned into 5-μm sections. The dysplasia and ESCC were determined and counted in the H&E-stained sections according to the following criteria: epithelial dysplasia confined to esophageal epidermis without obvious invasion, and the basement membrane was relatively intact (dysplasia); distinct invasion, unclearness, or loss of basement membrane; drop; and diffuse or extensive infiltration into the muscle layer (ESCC).

Statistical analysis

Error bars denote standard deviations (SDs). Two groups of independent samples were compared by two-sample t test. The results of the cell proliferation and cell migration experiments were analyzed using repeated-measures ANOVA. Protein expression data for esophageal carcinoma clinical tissue sections were analyzed using the chi-square test. Pearson's correlation was used for correlation analysis. For a test with a size of $\alpha = 0.05$, $p < 0.05$ was considered statistically significant (*$p < 0.05$, **$p < 0.01$, ***$p < 0.001$).

DATA AND CODE AVAILABILITY

Additional information is available at Molecular Therapy-Nucleic Acids's website (https://www.sciencedirect.com/journal/molecular-therapy-nucleic-acids). The accession number of raw sequencing data deposited to NCBI Gene Expression Omnibus (GEO) is GEO: GSE179267 (https://www.ncbi.nlm.nih.gov/geo/query/acc.cgi?acc=GSE179267).

SUPPLEMENTAL INFORMATION

Supplemental information can be found online at https://doi.org/10.1016/j.omtn.2021.07.007.

ACKNOWLEDGMENTS

This work was supported by grants from National Natural Science Foundation of China (81772999, 81974435, 81872409, and 81922052) and Natural Science Foundation of Guangdong Province (2019B151502011 and 2018A030313610).

AUTHOR CONTRIBUTIONS

D.C., Y.-Z.J., and S.L. conceived the study, designed the experiments, and supervised the project. H.H., C.Y., S.Z., M.C., S.G., Y.Z., J.M., Y.L., L.W., S.Z., and Z.W. performed the experiment and analyzed the data. H.H., D.C., and S.L. wrote the manuscript.

DECLARATION OF INTERESTS

The authors declare no competing interests.

REFERENCES

1. Reichenbach, Z.W., Murray, M.G., Saxena, R., Farkas, D., Karassik, E.G., Klochkova, A., Patel, K., Tice, C., Hall, T.M., Gang, J., et al. (2019). Clinical and translational advances in esophageal squamous cell carcinoma. Adv. Cancer Res. *144*, 95–135.
2. Yang, Y.M., Hong, P., Xu, W.W., He, Q.Y., and Li, B. (2020). Advances in targeted therapy for esophageal cancer. Signal Transduct. Target. Ther. *5*, 229.
3. Siegel, R.L., Miller, K.D., and Jemal, A. (2018). Cancer statistics, 2018. CA Cancer J. Clin. *68*, 7–30.
4. Bray, F., Ferlay, J., Soerjomataram, I., Siegel, R.L., Torre, L.A., and Jemal, A. (2018). Global cancer statistics 2018: GLOBOCAN estimates of incidence and mortality worldwide for 36 cancers in 185 countries. CA Cancer J. Clin. *68*, 394–424.
5. Gaur, P., Kim, M.P., and Dunkin, B.J. (2014). Esophageal cancer: Recent advances in screening, targeted therapy, and management. J. Carcinog. *13*, 11.
6. Peng, L., Cheng, S., Lin, Y., Cui, Q., Luo, Y., Chu, J., Shao, M., Fan, W., Chen, Y., Lin, A., et al. (2018). CCGD-ESCC: A Comprehensive Database for Genetic Variants Associated with Esophageal Squamous Cell Carcinoma in Chinese Population. Genomics Proteomics Bioinformatics *16*, 262–268.
7. Talukdar, F.R., di Pietro, M., Secrier, M., Moehler, M., Goepfert, K., Lima, S.S.C., Pinto, L.F.R., Hendricks, D., Parker, M.I., and Herceg, Z. (2018). Molecular landscape

of esophageal cancer: implications for early detection and personalized therapy. Ann. N Y Acad. Sci. *1434*, 342–359.

8. Gao, Y.B., Chen, Z.L., Li, J.G., Hu, X.D., Shi, X.J., Sun, Z.M., Zhang, F., Zhao, Z.R., Li, Z.T., Liu, Z.Y., et al. (2014). Genetic landscape of esophageal squamous cell carcinoma. Nat. Genet. *46*, 1097–1102.

9. Feng, Q., Zhang, H., Yao, D., Chen, W.D., and Wang, Y.D. (2019). Emerging Role of Non-Coding RNAs in Esophageal Squamous Cell Carcinoma. Int. J. Mol. Sci. *21*, E258.

10. Liu, J., Yue, Y., Han, D., Wang, X., Fu, Y., Zhang, L., Jia, G., Yu, M., Lu, Z., Deng, X., et al. (2014). A METTL3-METTL14 complex mediates mammalian nuclear RNA N6-adenosine methylation. Nat. Chem. Biol. *10*, 93–95.

11. Jia, G., Fu, Y., Zhao, X., Dai, Q., Zheng, G., Yang, Y., Yi, C., Lindahl, T., Pan, T., Yang, Y.G., and He, C. (2011). N6-methyladenosine in nuclear RNA is a major substrate of the obesity-associated FTO. Nat. Chem. Biol. *7*, 885–887.

12. Zheng, G., Dahl, J.A., Niu, Y., Fedorcsak, P., Huang, C.M., Li, C.J., Vågbø, C.B., Shi, Y., Wang, W.L., Song, S.H., et al. (2013). ALKBH5 is a mammalian RNA demethylase that impacts RNA metabolism and mouse fertility. Mol. Cell *49*, 18–29.

13. Yang, F., Jin, H., Que, B., Chao, Y., Zhang, H., Ying, X., Zhou, Z., Yuan, Z., Su, J., Wu, B., et al. (2019). Dynamic m^6A mRNA methylation reveals the role of METTL3-m^6A-CDCP1 signaling axis in chemical carcinogenesis. Oncogene *38*, 4755–4772.

14. Choe, J., Lin, S., Zhang, W., Liu, Q., Wang, L., Ramirez-Moya, J., Du, P., Kim, W., Tang, S., Sliz, P., et al. (2018). mRNA circularization by METTL3-eIF3h enhances translation and promotes oncogenesis. Nature *561*, 556–560.

15. Lin, S., Choe, J., Du, P., Triboulet, R., and Gregory, R.I. (2016). The m(6)A Methyltransferase METTL3 Promotes Translation in Human Cancer Cells. Mol. Cell *62*, 335–345.

16. Liu, L., Wu, Y., Li, Q., Liang, J., He, Q., Zhao, L., Chen, J., Cheng, M., Huang, Z., Ren, H., Chen, J., et al. (2020). METTL3 Promotes Tumorigenesis and Metastasis through BMI1 m6A Methylation in Oral Squamous Cell Carcinoma. Mol. Ther. *28*, 2177–2190.

17. Liu, J., Harada, B.T., and He, C. (2019). Regulation of Gene Expression by N^6-methyladenosine in Cancer. Trends Cell Biol. *29*, 487–499.

18. Huang, H., Weng, H., and Chen, J. (2020). m^6A Modification in Coding and Non-coding RNAs: Roles and Therapeutic Implications in Cancer. Cancer Cell *37*, 270–288.

19. Xia, T.L., Yan, S.M., Yuan, L., and Zeng, M.S. (2020). Upregulation of METTL3 Expression Predicts Poor Prognosis in Patients with Esophageal Squamous Cell Carcinoma. Cancer Manag. Res. *12*, 5729–5737.

20. Zhao, B.S., Roundtree, I.A., and He, C. (2017). Post-transcriptional gene regulation by mRNA modifications. Nat. Rev. Mol. Cell Biol. *18*, 31–42.

21. Yao, M.D., Jiang, Q., Ma, Y., Liu, C., Zhu, C.Y., Sun, Y.N., Shan, K., Ge, H.M., Zhang, Q.Y., Zhang, H.Y., Yao, J., et al. (2020). Role of METTL3-Dependent N6-Methyladenosine mRNA Modification in the Promotion of Angiogenesis. Mol. Ther. *28*, 2191–2202.

22. Fang, X., Li, M., Yu, T., Liu, G., and Wang, J. (2020). Reversible N6-methyladenosine of RNA: The regulatory mechanisms on gene expression and implications in physiology and pathology. Genes Dis. *7*, 585–597.

23. Jin, H., Ying, X., Que, B., Wang, X., Chao, Y., Zhang, H., Yuan, Z., Qi, D., Lin, S., Min, W., et al. (2019). N^6-methyladenosine modification of ITGA6 mRNA promotes the development and progression of bladder cancer. EBioMedicine *47*, 195–207.

24. Jin, D., Guo, J., Wu, Y., Du, J., Yang, L., Wang, X., Di, W., Hu, B., An, J., Kong, L., et al. (2019). m^6A mRNA methylation initiated by METTL3 directly promotes YAP translation and increases YAP activity by regulating the MALAT1-miR-1914-3p-YAP axis to induce NSCLC drug resistance and metastasis. J. Hematol. Oncol. *12*, 135.

25. Shi, Y., Zheng, C., Jin, Y., Bao, B., Wang, D., Hou, K., Feng, J., Tang, S., Qu, X., Liu, Y., et al. (2020). Reduced Expression of *METTL3* Promotes Metastasis of Triple-Negative Breast Cancer by m6A Methylation-Mediated *COL3A1* Up-Regulation. Front. Oncol. *10*, 1126.

26. Liu, X., Gonzalez, G., Dai, X., Miao, W., Yuan, J., Huang, M., Bade, D., Li, L., Sun, Y., and Wang, Y. (2020). Adenylate Kinase 4 Modulates the Resistance of Breast Cancer Cells to Tamoxifen through an m6A-Based Epitranscriptomic Mechanism. Mol. Ther. *28*, 2593–2604.

27. Majumder, S., Crabtree, J.S., Golde, T.E., Minter, L.M., Osborne, B.A., and Miele, L. (2021). Targeting Notch in oncology: the path forward. Nat. Rev. Drug Discov *20*, 125–144.

28. Li, Y., Li, Y., and Chen, X. (2021). NOTCH and Esophageal Squamous Cell Carcinoma. Adv. Exp. Med. Biol. *1287*, 59–68.

29. Natsuizaka, M., Whelan, K.A., Kagawa, S., Tanaka, K., Giroux, V., Chandramouleeswaran, P.M., Long, A., Sahu, V., Darling, D.S., Que, J., et al. (2017). Interplay between Notch1 and Notch3 promotes EMT and tumor initiation in squamous cell carcinoma. Nat. Commun. *8*, 1758.

30. Lubin, D.J., Mick, R., Shroff, S.G., Stashek, K., and Furth, E.E. (2018). The notch pathway is activated in neoplastic progression in esophageal squamous cell carcinoma. Hum. Pathol. *72*, 66–70.

31. Lin, S., Liu, Q., Lelyveld, V.S., Choe, J., Szostak, J.W., and Gregory, R.I. (2018). Mettl1/Wdr4-Mediated m^7G tRNA Methylome Is Required for Normal mRNA Translation and Embryonic Stem Cell Self-Renewal and Differentiation. Mol. Cell *71*, 244–255.e5.